ce/papers Proceedings in civil engineering

Ernst & Sohn A Wiley Brand

Full paper

Strain Limit in Structural Steel Joint Analysis

Kirill Golubiatnikov[1] | František Wald[1] | Martin Vild[2]

Correspondence

Mgr. Kirill Golubiatnikov, Ph.D.
Czech Technical University in Prague
Department of Steel and Timber Structures
Thakurova 2077/7
166 29 Prague, Czechia
Email: kirill.golubiatnikov@fsv.cvut.cz

[1] Czech Technical University in Prague, Prague, Czechia
[2] Brno University of Technology, Brno, Czechia

Abstract

Inelastic numerical analysis is a classic method in engineering practice. Failure criteria are primarily expressed in terms of plastic strain limits. Several factors influence the plastic strain limit, including material properties, element geometry, numerical element type, mesh density, and constitutive relations.

Component-Based Finite Element Method (CBFEM) is a widely used technique for the design of steel connections. It combines the analytical component method with the numerical finite element method (FEM). FEM is used to determine the distribution of internal forces, and plates are modeled using 4-node shell elements. Connection components are replaced by dependent nonlinear springs and analysis models derived from their specific behavior.

This paper presents the results of determining the plastic strain limit for CBFEM numerical calculations. The limit is presented as a reduced value of the ultimate strain. The partial safety factor was determined for nine geometries of weakened plates based on design values obtained from Monte Carlo simulation and reliability analysis. The Monte Carlo simulation was performed using a combination of FEM analysis and analytical formulas implemented in Python. The plastic strain limit was found to be 4.77% over all mesh densities.

Keywords

Structural steel, Inelastic analyses, Strain limit, Component Based Finite Element method

1 Introduction

The load-bearing capacity of weakened cross-section structures made from structural steels, i.e. with yield strength f_y up to 500 MPa, is limited by the onset of necking. The load-bearing capacity is more appropriately expressed as the design equivalent plastic strain limit $\varepsilon_{R,d}$ in Finite Element Method (FEM) numerical analysis. The equivalent plastic strain represents the accumulated local plastic deformations during the simulation process [1]. Solonick in [2] and FprEN 1993-1-14 [3] expressed the equivalent plastic strain limit $\varepsilon_{R,d}$ as reduction value of the ultimate strain ε_u by partial safety factor γ_X:

$$\varepsilon_{R,d} = \gamma_X \varepsilon_u \qquad (1)$$

$$\varepsilon_u = 0.6(1 - f_y/f_u) \text{ but } \varepsilon_u \geq 0.06 \qquad (2)$$

where ε_u is the guaranteed minimum ultimate strain, which is recommended to be calculated as a function of the yield f_y to ultimate strength f_u ratio [4]. Partial safety factor γ_X must decrease the ultimate strain up to the limit value, when the corresponding resistance N_R equals or is smaller than design net cross-section resistance $N_{R,d}$. The project FprEN 1993-1-1 [5] recommends using the following equation for design calculations:

$$N_{R,d}^{EN} = A_{net} f_u / \gamma_{M2} \qquad (3)$$

Here, $A_{net} f_u$ represents the average ultimate resistance of an element with the nominal net cross-section area A_{net} and the ultimate strength f_u. This dependence highlights the importance of material properties M and geometry G for resistance. The real structure geometry, such as global element sizes, hole positions, etc., and steel material properties are diverse. The partial safety factor for resistance in tension γ_{M2} accounts for this variability and statistically guarantees that the design standard net cross-section resistance in numerical calculation $N_{R,d}^{EN}$ is smaller

https://doi.org/10.1002/cepa.70176 wileyonlinelibrary.com/journal/cepa

than 99.89 % of possible design real net cross-section resistances $N_{\mathrm{R}}^{\mathrm{r}}$ [6], i.e $N_{\mathrm{R,d}}^{\mathrm{EN}} \leq N_{\mathrm{R,d}}^{\mathrm{r}}$. Therefore, Equation (3) can be rewritten statistically as follows: [7]:

$$N_{\mathrm{R,d}}^{\mathrm{EN}} \leq N_{\mathrm{R,d}}^{\mathrm{r}} = n\, N_{\mathrm{R}}^{\mathrm{r}}\{M,G,U\} - 0.0011n\, N_{\mathrm{R}}^{\mathrm{r}}\{M,G,U\} \qquad (4)$$

where $n\, N_{\mathrm{R}}^{\mathrm{r}}\{M,G,U\}$ represents the database of possible real resistances with n number of samples, $0.0011n\, N_{\mathrm{R}}^{\mathrm{r}}\{M,G,U\}$ represents 0.11 % of the sample database, which could be on the unsafe side. The uncertainty factor U in the possible real resistance $N_{\mathrm{R}}^{\mathrm{r}}\{M,G,U\}$ accounts for the variability in material properties and geometry.

The partial safety factor γ_{X} must be valid for numerical design calculations according to European standards. This type of FEM analysis should performed with nominal geometry, nominal material properties from Tables 5.1, 5.2 in FprEN 1993-1-1 [5] and material models in Engineering stress-strain format from section 5.3.2 in FprEN 1993-1-14 [3]. Nominal material properties are the lowest statistically guaranteed values.

The standard ultimate resistance in numerical design calculation $A_{\mathrm{net}} f_{\mathrm{u}}^{\mathrm{EN}}$ can be significantly lower than the real ultimate resistance. It is incorrect and overly conservative to use the same partial safety factor γ_{M2} in numerical design calculation, which was determined experimentally or through simulations with real material properties. Therefore, the design real net cross-section resistance, determined by the First Order Reliability Method (FORM) or the Deformation Energy Ratio approach (DER), should be used. The calculation of the design resistance according to the FORM method is shown in Equation (4). The DER approach was first presented in [8]. In this approach, the area under Force – Deformation curves up to the ultimate resistance represents the deformation energy E_{u}, which is required to reach the ultimate resistance. Similarly, E_{R} is the deformation energy required to reach the design resistance $N_{\mathrm{R,d}}$. In both cases, real simulations and design standard calculation, their ratios must be the same. The design real net cross-section resistance $N_{\mathrm{R,d}}^{\mathrm{r}}$ is a real resistance, while the design DER ratio $E_{\mathrm{R}}^{\mathrm{r}}/E_{\mathrm{u}}^{\mathrm{r}}$ is an idealized ratio. In the end, design standard net cross-section resistance $N_{\mathrm{R,d}}^{\mathrm{EN}}$ can be taken as one of the two options, whose were calculated statistically according to Equation (4):

$$N_{\mathrm{R,d}}^{\mathrm{EN}} = \begin{cases} N_{\mathrm{R,d}}^{\mathrm{r}}, & \text{if } N_{\mathrm{R,d}}^{\mathrm{r}} \leq A_{\mathrm{net}} f_{\mathrm{u}}^{\mathrm{EN}} \\ N_{\mathrm{R,d}}^{\mathrm{DER}} \rightarrow E_{\mathrm{R}}^{\mathrm{EN}} / E_{\mathrm{u}}^{\mathrm{EN}} = E_{\mathrm{R}}^{\mathrm{r}} / E_{\mathrm{u}}^{\mathrm{r}} \end{cases} \qquad (5)$$

The main goal of this work is the determination of the partial safety factor γ_{X} for numerical standard design calculations according to the Component-Based Finite Element Method (CBFEM). Ultimate strain should calculate using Equation (2). The design standard equivalent plastic strain limit $\varepsilon_{\mathrm{R,d}}$ is the maximum plastic strain in element at the design standard net cross-section resistance $N_{\mathrm{R,d}}^{\mathrm{EN}}$. It is apparent that plastic strains depend also on the numerical model variables. These variables and their influences on the plastic strain limit at the design analytical resistance, see Equation (1), were studied in [9] and [10]. The material model used had the most influence. The analyses with the most realistic model had lower plastic strain limits. Based on this, the linear elastic – linear hardening plastic material model [3] was selected for this work.

The next important variables were the numerical element type and mesh density. Since determining the maximum strain on a weakness edge is very similar to determining the structural stress on the concentrator edge, the Hot Spot Stress Method guide from International institute of welding [11] can be applied. Numerical elements are classified into solid and shell elements. Using solid linear 4-node tetrahedron is forbidden. A 10-node tetrahedron can be used with a reasonably fine element mesh near concentrator, although it is almost impossible to apply it effectively. The cubic 20-node and 8-node elements can be used as solid elements, while quadrilateral 8-node and 4-node elements can be selected as shell elements. In this work, only the 4-node (Shell 4nd) element was used, because this numerical element is recommended for the CBFEM method. According to this guide, mesh density is divided into coarse meshes with element sizes greater than $0.4t_{\mathrm{n}} \times 0.4t_{\mathrm{n}}$, and fine meshes with element sizes up to $0.4t_{\mathrm{n}} \times 0.4t_{\mathrm{n}}$. The mesh sizes $1t_{\mathrm{n}} \times 1t_{\mathrm{n}}$, $0.5t_{\mathrm{n}} \times 0.5t_{\mathrm{n}}$, $0.25t_{\mathrm{n}} \times 0.25t_{\mathrm{n}}$ and $0.2t_{\mathrm{n}} \times 0.2t_{\mathrm{n}}$ were chosen based on the results in [10]. The deflection theory had the least influence on the plastic strain limits in [9], but values from analyses with small deflection theory were always smaller. Therefore, the small deflection theory was used in all numerical standard calculations.

2 Design real values

The design real values are the design real net cross-section resistance $N_{\mathrm{R,d}}^{\mathrm{r}}$ and the design real DER ratio $E_{\mathrm{R}}^{\mathrm{r}}/E_{\mathrm{u}}^{\mathrm{r}}$. Both values must be determined according to reliability procedure from Annex C of EN 1990 [6], as presented in Equation (4). The database of the possible resistances $n\, N_{\mathrm{R}}^{\mathrm{r}}\{M,G,U\}$ was created by the Monte Carlo simulation. The number of samples n was set to 3 500 000 for each selected geometry type. The possible resistance $N_{\mathrm{R}}^{\mathrm{r}}\{M,G,U\}$ was calculated by the numerical-analytical net cross-section resistance model. In the final step, the obtained design real net cross-section resistances $N_{\mathrm{R,d}}^{\mathrm{r}}$ were sorted according to the initial stress concentration factor SCF_{i} and the ultimate to yield strength ratio $f_{\mathrm{u}}/f_{\mathrm{y}}$ of the used material model.

2.1 Inputs

The first input is material properties M. The distributions of the real material properties for European steels were presented in [12]. The occurrence frequencies of yield strength f_{y} and ultimate f_{u} strength must remain consistent with the original distribution, meaning they are pseudorandom values. Structural steel must meet the ductility requirement $f_{\mathrm{u}}/f_{\mathrm{y}} = 1.1$ as per 5.2.2(a) of FprEN 1993-1-1 [5]. The combinations of material properties, along with the ductility requirement, are shown in Figure 1a).

The real ultimate resistances $A_{\mathrm{net}} f_{\mathrm{u}}$ and Force-Deformation curves were established numerically. Solving numerical models for all possible combinations of material properties is not feasible. Therefore, all combinations were grouped into six $f_{\mathrm{u}}/f_{\mathrm{y}}$ ratios: 1.1, 1.2, 1.3, 1.4, 1.5 and 1.6, separated according to classical mathematical rules. The resulting relative frequencies are presented in Figure 1b).

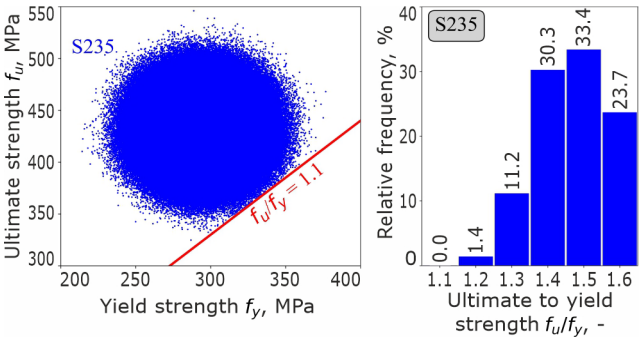

Figure 1 Material properties input: real values with ductility requirement (left) and simplified distribution (right)

The second input is geometry G. Nine geometry types with different concentrator configurations – such as notches, holes or slotted holes - were selected for this analysis, as shown in Figure 2. All types have the same net cross-section area, meaning they have the same analytical resistances according to Equation (3). The maximum weakening was taken based on the minimum edge distance from EN 1993-1-8 [13], as in the case of a plate with single central hole:

$$w = 2e_2 = 2.4d \rightarrow d = w/2.4 = 0.417w \qquad (6)$$

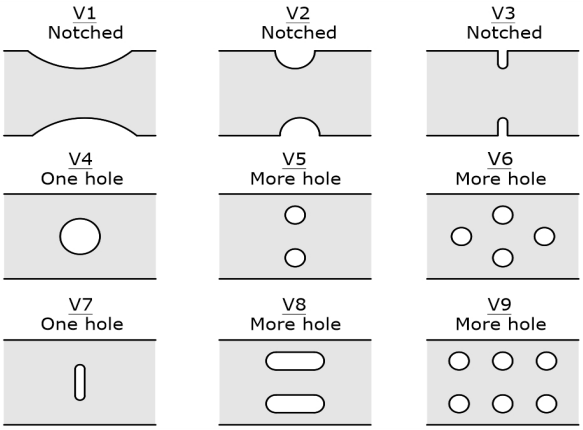

Figure 2 Geometry input – geometry types

The concentrator configurations cause changes in stress and strain fields. Those changes can be expressed by the Stress concentration factor SCF, which represents the ratio of the stress peak σ_{max} at the concentrator edge to the nominal stress σ_{nom} in the element. The nominal stress can be taken either from the analytical equation N/A or as a value from the numerical model at the location that is not influenced by the stress peak caused by geometry changes or boundary conditions. Since the SCF factor varies during the loading process, the initial stress concentration factor SCF_i in the elastic part up to the yield strength was used for this work:

$$SCF_i = \sigma_{max}/\sigma_{nom} \qquad (7)$$

The next geometry property is thickness. The real thickness may vary from the nominal value and can be also described by statistical distributions, which can be used to generate pseudorandom values. These distributions for European steel elements were studied in [12]. An element can be calculated according to European standards if its real thickness t_r is within the limited range of possible deviations. Extreme permitted thickness deviations for hot-rolled plates are shown in EN 10029 [14]. The largest deviations occur for a nominal thickness of 5 mm and therefore, $t5$ was selected for this study. The used distribution with its boundary conditions is presented in **Figure 3**.

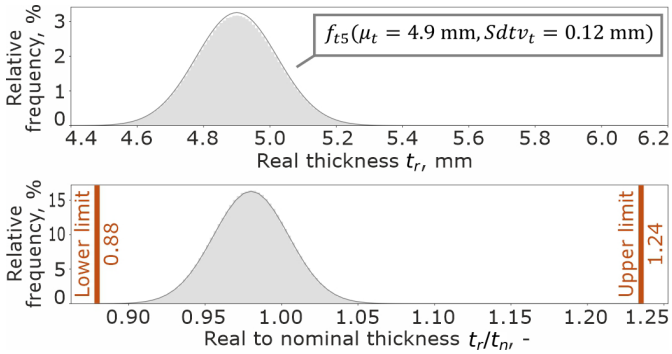

Figure 3 Geometry input – real thickness

The last geometry property is the functional tolerances of concentrator production. It is impossible to produce all concentrators identically. Holes may have small deviations in their locations and could exhibit slight ovality. Additionally, the minimum radius for a concentrator is also limited. All permitted functional tolerances are described in EN 1090-2 [15] and the used tolerances are shown in Figure 4. European standards do not apply to more extreme tolerances.

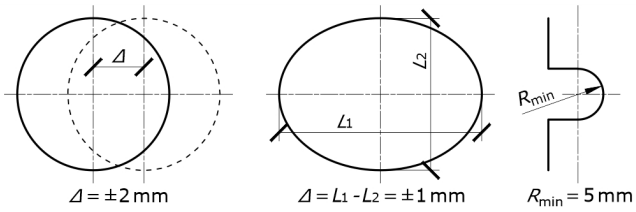

Figure 4 Geometry input – extreme permitted functional tolerances

2.2 Net cross-section resistance model

Resistance $N_R^r\{M, G, U\}$ represents the real ultimate resistance for an element with material properties input M and geometry input G. Therefore, the Eurocode resistance Equation (3) were taken with a slight modification. The partial safety factor γ_{M2} is replaced by the combination factors:

$$N_R^r\{M, G, U\} = A_{net} f_u^r \, G_t U \qquad (8)$$

where $A_{net} f_u^r$ is the numerically determined real ultimate resistance from the numerical simulation with perfect geometry, i.e. without of functional tolerances and nominal thickness; G_t is the reduction factor of real thickness and U is uncertainty factor.

The influence of different inputs was studied through numerical simulations performed in Ansys 2022 R2 using the Static Structural module. The simulations were conducted using Solid 20nd numerical elements with mesh density of $0.2t_n \times 0.2t_n$. The linear elastic – linear hardening plastic material model, as described in 5.3.2c) of FprEN 1993-1-14 [3], was used. The statistically guaranteed minimum ultimate strength f_u from the real distributions [12] was

determined according to Annex C of EN 1990 [6] for normal distribution and equals 372.9 MPa. The yield strength f_y was chosen to maintain the required f_u/f_y ratio. Since it is not feasible to perform simulations for each possible f_u/f_y ratio, only the ratios 1.1, 1.2, 1.3, 1.4, 1.5 and 1.6 were considered. The material model in Ansys was defined using Isotropic Elasticity tool for the elastic part and Multilinear Isotropic Hardening tool for the inelastic part. The numerical modelling procedure was validated in [9] and [10]. Simulations for each geometry type were solved with various combinations of extreme functional tolerances and thickness deviation. The obtained ultimate resistances from numerical simulation with perfect geometry were used as real ultimate resistances $A_{net}f_u^r$.

The reduction factor of real thickness G_t was determined based on the simulation results and was used to decrease the real ultimate resistance $A_{net}f_u^r$ to the lowest resistance for the assessed geometry type and real to nominal thickness ratio t_r/t_n, as presented in Figure 5.

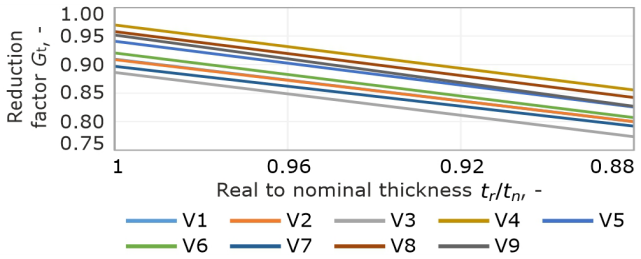

Figure 5 Reduction factor of real thickness G_t

The material model used represents statistically guaranteed the lowest material properties, as Yun and Gardner demonstrated in [4]. Moreover, not every element must have the worst functional tolerances. Therefore, the uncertainty factor U increases the lowest real resistance, $A_{net}f_u^r\,G_t$, to a value within a range from 1 to 1.191, as shown in Figure 6. This distribution was prepared by comparing the numerical-analytical resistances according to this approach, Equation (8) with experimental resistances from [9], [16] and [7]. The upper limit of factor U was set to the maximum obtained value.

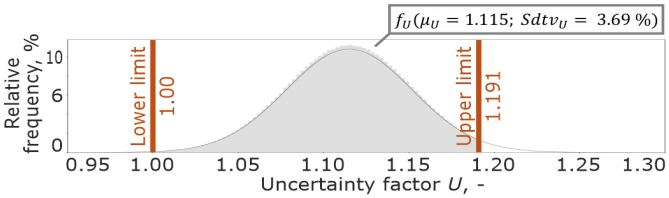

Figure 6 Uncertainty factor U

2.3 Results

A determination of the real net cross-section resistance $N_R^r\{M,G,U\}$, as shown in Equation (8), was repeated $n = 3500000$ times with pseudorandom values of the material properties M, geometry G and uncertainty factor U. Subsequently, the deformation energies E_R^r, E_u^r and their ratio using the DER approach were calculated based on the Force-Deformation curves from the numerical simulations with perfect geometry. The obtained databases of real resistances and DER ratios were evaluated according to Equation (4) and the design real net cross-section resistance $N_{R,d}^{FORM}$ and design real DER ratio E_R^r/E_u^r were determined.

If the ultimate f_u to yield f_y strength ratio of the steel used is small, the resistance is high, while the corresponding deformation is small, as seen in high-strength steels. Conversely, as the f_u/f_y ratio increases, the resistance decreases while the corresponding deformation increases. This indicates that resistance and deformation are interdependent. The Deformation Energy Ratio approach takes this into account. The design real net cross-section resistances $N_{R,d}^r$ for each considered f_u/f_y ratio were calculated based on the design real DER E_R^r/E_u^r ratio. The design resistance $N_{R,d}^r$ cannot be lower than the design real resistance calculated by the FORM method $N_{R,d}^{FORM}$ according to Equation (4) [6]. If the design real DER resistance $N_{R,d}^{DER}$ was smaller than design FORM resistance $N_{R,d}^{FORM}$, then the FORM resistance was accepted as the design real resistance $N_{R,d}^r$. An example of the results is presented for geometry type V1 in Figure 7. This mean that the design real net cross-section resistance $N_{R,d}^r$ always equals the design real resistance according to FORM method $N_{R,d}^{FORM}$. However, if the f_u/f_y ratio is known, as in the case of existing structures, the design real net cross-section resistance $N_{R,d}^r$ can be increased and determined using the DER approach.

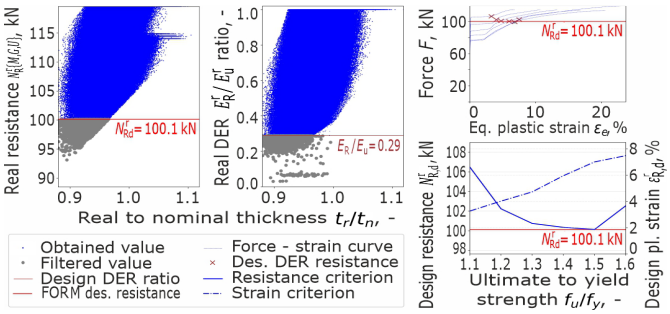

Figure 7 Determination of the design real net cross-section resistance and design real deformation energy ratio for geometry type V1

The described approach was applied to all 9 geometry types presented in **Figure 2**. The obtained design real net cross-section resistances $N_{R,d}^r$ were sorted according to the initial stress concentration factor SCF_i and the ultimate to yield strength ratio f_u/f_y of the used material model, see Figure 8. The lowest resistances were determined for geometry type V7, because its ultimate resistances $A_{net}f_u^r$ were also the smallest. The design real resistance $N_{R,d}^r$ decreases as either ultimate to yield strength ratio or initial stress concentration factor increases.

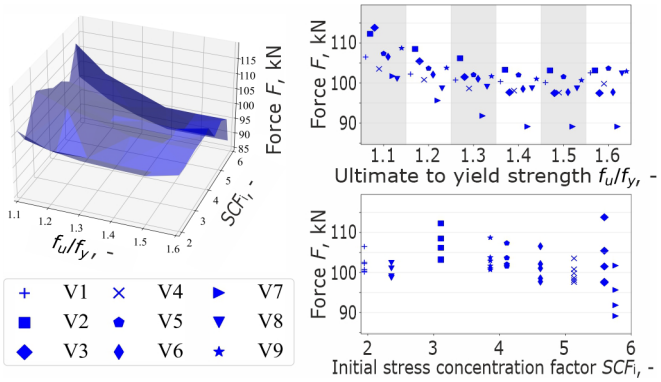

Figure 8 Design real net cross-section resistances $N^{r}_{R,d}$ for steel S235

3 Design standard values

As stated in the introduction, the equivalent plastic strain limit is a better limiting parameter for numerical analysis. The design standard equivalent plastic strain limit $\varepsilon_{R,d}$ corresponds to the design standard net cross-section resistance $N^{EN}_{R,d}$. Both design standard values depend on the geometry of an element and, more importantly, on the mechanical properties of material. Using a constant equivalent plastic strain limit for all structural steels is conservative, because it would represent only the lowest limit. Therefore, presenting the limit as a reduction value of the ultimate strain, as shown in Equation (1), is a more advanced approach.

The engineering material model in numerical design calculation must employ the nominal material properties from FprEn 1993-1-1 [5]. In the work, they were combined with the linear elastic – linear hardening plastic material model [3]. The achieved material model is shown in Figure 9. The statistically guaranteed ultimate strain ε_u is a constant value of 20.8 % according to Equation (2) and [4].

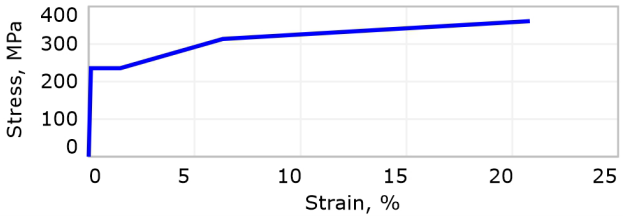

Figure 9 Engineering material model of S235 steel

The design standard net cross-section resistance $N^{EN}_{R,d}$, as shown in Equation (5), can be taken as either the design real net cross-section resistance $N^{r}_{R,d}$, if the standard ultimate resistance in numerical calculation $A_{net}f^{EN}_{u}$ is smaller than $N^{r}_{R,d}$, or the design resistance $N^{DER}_{R,d}$ based on the design real DER ratio E^{r}_{R}/E^{r}_{u}. The deformation caused by the applied force in the numerical analysis primarily depends on the numerical element type and mesh size, while the deflection theory has almost negligible influence. Therefore, the design standard resistance $N^{EN}_{R,d}$ was determined based on the Force-Deformation curve, which was solved with the Solid 20nd numerical elements and mesh density $0.2t_n \times 0.2t_n$. Only the material model was replaced with the engineering material model from Figure 9. An example of the approach is presented in Figure 10, left figure.

Subsequently, the standard equivalent plastic strain limits $\varepsilon_{R,d}$ were determined based on the Force-Equivalent plastic strain curves from numerical calculations, which had various mesh density. The 4-node elements were used. The mesh sizes $1t_n \times 1t_n$, $0.5t_n \times 0.5t_n$ were selected as coarser mesh densities, while $0.25t_n \times 0.25t_n$ and $0.2t_n \times 0.2t_n$ were chosen as finer mesh densities. All numerical calculations were performed with the Small deflection theory. The standard equivalent plastic strain limit $\varepsilon_{R,d}$ for each numerical calculation was accepted as a corresponding plastic strain at the design standard net cross-section resistance $N^{EN}_{R,d}$. The achieved equivalent plastic strain limits for geometry type V1 are shown in Figure 10, right figure.

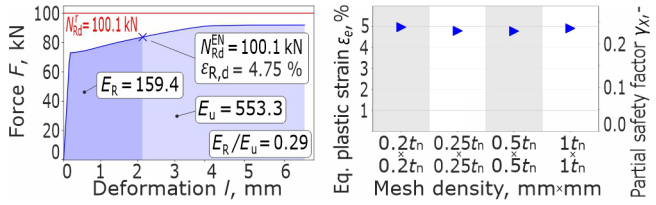

Figure 10 Determination of the design standard net cross-section resistance $N^{EN}_{R,d}$ (left) and the equivalent standard plastic strain limit $\varepsilon_{R,d}$ (right) for numerical calculations. Geometry type V1

Together, the partial safety factor γ_X was calculated by dividing the equivalent plastic strain limit $\varepsilon_{R,d}$ by the guaranteed ultimate strain ε_u for steel S235, i.e. $\varepsilon_{R,d}/20.8\,\%$. The achieved values for all geometry types are sorted according to the initial stress concentration factor SCF_i, color-coded according to concentrator configurations and presented in Figure 11. Geometry type names are added on the upper axis for better orientation. The coarser mesh densities have lower limit values and, in this case, the linear constant limit is sufficient. For finer meshes, the limit can be expressed by an advanced approximation function depending on the initial stress concentration factor SCF_i. It should be noted that only geometry type V3 was calculated with the design real net cross-section resistance $N^{r}_{R,d}$, i.e. the real resistance. The design resistances for the other geometry types were determined with the idealized resistances according to the DER approach. Therefore, the achieved partial safety factor γ_X can be a bit increased.

The critical values were obtained with geometry type V1, which presents a relatively smooth notch. Although its design real net cross-section resistance $N^{r}_{R,d}$ and design real DER ratio E^{r}_{R}/E^{r}_{u} were not the lowest, as shown in Figure 8 and Figure 7, this geometry type does not cause significant strain peaks at the concentrator edge. In contrast, geometry type V3 exhibits sharp increases in plastic strain even with small force changes. In almost all cases, a decrease in the concentrator radius exhibits an increase in the equivalent plastic strain limit. Conversely, the limit from the numerical calculation with a mesh density $1t_n \times 1t_n$ shows a decrease, due to the pooper quality of the edge meshing. The transition from a hole to a slotted longitudinal hole - geometry types V5 and V8 - results in a reduction of the strain peak at the hole edge. As a result, the final concentrator configuration begins to resemble a relatively smooth concentrator. The addition of staggered holes, geometry type V6, decreases the equivalent plastic strain limit, while the addition of in-line holes increases the limit.

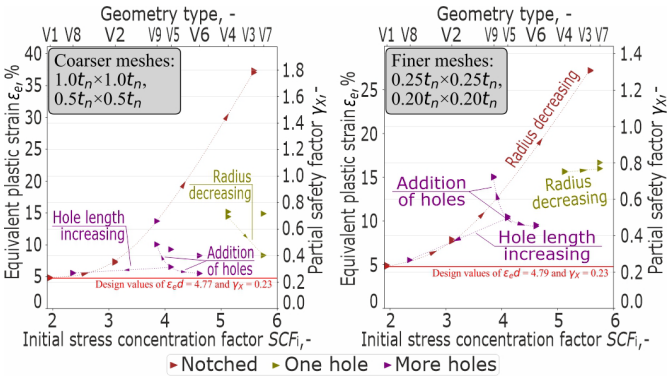

Figure 11 Achieved partial safety factors γ_X for numerical calculation according to CBFEM with coarse meshes (left) and fine meshes (right)

4 Conclusion

In this paper, the design equivalent plastic strain limit $\varepsilon_{R,d}$ was determined for numerical calculations using the Component Based Finite Element Method. The limit was represented as a reduced value of the ultimate strain ε_u. The Partial safety factor γ_X was determined for nine geometries of weakened plates based on design values, which were obtained by Monte Carlo simulation and reliability analysis according to Annex C of EN 1990 [6]. The Monte Carlo simulation was performed using a combination of FEM analysis and analytical formulas implemented in Python. The main conclusions are:

- Plastic strain limit was determined to be 4.77% across all mesh densities.
- Lowest design real net cross-section resistance was determined with geometry type V7.
- Design real net cross-section resistance $N_{R,d}^{r}$ always equals the design real resistance according to First Order Reliability Method $N_{R,d}^{FORM}$, but if the f_u/f_y ratio is known, as in the case of existing structures, the design real net cross-section resistance $N_{R,d}^{r}$ can be increased and determined using the Deformation Energy Ratio approach.
- Critical design equivalent plastic strain limit $\varepsilon_{R,d}$ were obtained with geometry type V1, which presents a relatively smooth notch.
- Decrease in the concentrator radius results in an increase in the equivalent plastic strain limit. Conversely, the limit from the numerical calculation with a mesh density $1t_n \times 1t_n$ shows a decrease, due to the poor quality of the edge meshing.
- Transition from a hole to a slotted longitudinal hole results in a reduction of the strain peak at the hole edge. The addition of staggered holes reduces the equivalent plastic strain limit, while the addition of in-line holes increases this limit.

This study was supported by project of Ministry of Education, Youth and Sports Inter Excellence LUAUS23114.

References

[1] Zheng, J.; Shu, X.; Wu, Y.; Xu, H.; Lu, Q.; Liao, B.; Zhang, B. (2018) *Investigation on the plastic deformation during the stamping of ellipsoidal heads for pressure vessels*. Thin-Walled Structures 127, pp. 135-144. https://doi.org/10.1016/j.tws.2018.01.040.

[2] Solonick, W. (1996) *Elastic-plastic strain acceptance criterion for structures subject to rapidly applied transient dynamic loading*. *Report KAPL-P-000034 (K96014)*. New York:U.S. department of Energy.

[3] FprEn 1993-1-14 (2025): *Design of steel structures — Part 1-14: Design assisted by finite element analysis*.

[4] Yun, X., Gardner, L. (2017) *Stress-strain curves for hot-rolled steels*. Journal of construction steel research 133, pp. 36-46. https://doi.org/10.1016/j.jcsr.2017.01.024.

[5] FprEn 1993-1-1 (2022): *Design of steel structures — Part 1-1: General rules and rules for buildings*.

[6] EN 1990 ed.2 (2002): *Eurocode - Basic of structural design*.

[7] Snijder, HH.; Dekker, RWA.; Teeuwen, PA. *Net cross-section failure of steel plates at bolt holes: numerical work and statistical assessment of design rules*. ce/papers 1, No. 2&3, pp. 3679-3688. https://doi.org/10.1002/cepa.424.

[8] Golubiatnikov, K.; Wald, F. (2025) *Conversion between the numerical simulation and the calculation using the Deformation Energy Ratio approach*. MethodsX 14, pp. 103221. https://doi.org/10.1016/j.mex.2025.103221.

[9] Golubiatnikov, K.; Ghimire, A.; Wald, F.; Stančík, V. (2025) *Determination of design plastic strain limit for notched structural steel tensile specimens*. Alexandria Engineering Journal 121, pp. 38-52. https://doi.org/10.1016/j.aej.2025.02.075.

[10] Golubiatnikov, K.; Ghimire, A.; Wald, F.; Vild, M. (2024) *Limit Strain in the Elastic-Plastic Analysis in Steel*. Nordic Steel Construction Conference 2024. https://doi.org/10.5281/zenodo.11449395.

[11] Niemi, E.; Fricke, W.; Maddox, SJ. (2018) *The structural hot-spot stress approach to fatigue analysis of welded components. Designer´s guide*. Singapore: Springer Nature Singapore Pre Ltd.

[12] Simões da Silva, L.; Marques, L.; Tankova, T.; Rebelo, C.; Kuhlmann, U.; Kleiner, A.; Spiegler, J.; Snijder, HH.; Dekker, RWA.; Dehan, V.; Taras, A.; Haremza, C.; Cajot, LG.; Vassart, O.; Popa, N. (2015) *Standardization of Safety Assessment Procedures across Brittle to Ductile Failure Modes (SAFEBRICTILE). Final report*. Directorate-General for Research and Innovation.

[13] EN 1993-1-8 (2005): *Design of steel structures — Part 1-8: Design of joints*.

[14] EN 10029 (2010): *Hot-rolled steel plates 3 mm thick or above - Tolerances on dimensions and shape*.

[15] EN 1090-2 (2018): *Execution of steel structures and aluminium structures - Part 2: Technical requirements for steel structures*.

[16] Romanowicz, P.; Szybinski, B.; Wygoda, M.

(2020) *Application of DIC Method in the Analysis of Stress Concentration and Plastic Zone Development Problems*, Materials 13(16), 3460. https://doi.org/10.3390/ma13163460.